TORSO DEFORMATION IN FRONTAL SLED TESTS: COMPARISION BETWEEN THOR NT, THOR NT WITH THE CHALMERS SD-1 SHOULDER, AND PMHS

G. Shaw, D. Parent, S. Purtsezov, D. Lessley, J. Crandall
Center for Applied Biomechanics
University of Virginia

F. Törnvall
Chalmers University of Technology

ABSTRACT

This study compares the thoracic deformation response of the 50th percentile male THOR NT frontal crash dummy and the response of the THOR modified with the SD-1 shoulder (THOR SD-1) relative to the thoracic response of eight 50th percentile male PMHS. The prototype Chalmers University SD-1 shoulder was designed to be more human-like in terms of geometry and range of motion in comparison to the standard THOR NT shoulder. The dummies and PMHS were restrained by a three-point restraint in a driver-side configuration and were subjected to a simulated 40 km/h frontal crash. The most prominent difference between the responses of the dummies and PMHS involved motion of the lower right anterior ribcage measurement site that is the farthest lateral distance from the diagonal shoulder belt. During the impact event, this site moved substantially anteriorly and away from the spine for the PMHS. The PMHS lower right "bulge out" behavior is believed to be caused by inertial loading of the ribcage, underlying organs, and soft tissue overlying the torso. The THOR SD-1 shoulder altered the shoulder belt position relative to the thoracic deflection measurement sites resulting in a different distribution of deformation for the upper measurement sites although the average upper site deformation was similar to that recorded for the standard THOR shoulder.

Key Words: Thorax deformations, Dummies, Shoulder, Cadavers, Frontal Impacts

INJURIES TO THE CHEST are a major source of morbidity and mortality in motor vehicle crashes (Nirula and Pintar 2008), especially for older occupants (Morris et al. 2002; Kent et al. 2005). Since the early 1960s, the goal of reducing chest injuries has motivated numerous studies of human thoracic response to loading. Restraint loading of the anterior chest in frontal crashes continues to be a major source of occupant injury. In frontal crashes, the magnitude of thoracic deformation due to anterior chest loading is commonly used as an indicator of rib and sternal fracture risk. These fractures are the most frequently observed thoracic injury in occupants loaded by contemporary restraint systems (Kent et al. 2003).

Three-point belt systems, a nearly universal standard component of contemporary restraint systems, deform the torso by loading the shoulders and the ribcage (Figure 1). A significant percentage of the restraint load borne by the shoulders reduces the load, deformation, and injury sustained by the ribcage. Effective restraint systems employ this "shoulder shielding" mechanism (Schneider et al 1992). Therefore, a frontal crash dummy is most effective as a restraint design tool when the apportionment of restraint loads between the shoulders and the ribcage is human-like. One of the objectives the THOR (Test device for Human Occupant Restraint) dummy development effort was to improve shoulder biofidelity compared to the Hybrid III, a goal considered by the developers to be as important as that for the chest and abdomen (Schneider et al 1992). Although the shoulder design of the THOR is more human-like than that of the Hybrid III, compromises were made in its design due primarily to manufacturing and durability considerations. In addition, the developers were limited by a lack of human shoulder kinematic data in a frontal crash environment (Schneider et al 1992).

Examining the shoulder geometry, the location of THOR's clavicle is somewhat different compared to that of a similarly sized human (Figure 2). This motivated an evaluation of a new THOR shoulder, the Chalmers University SD-1 (Figure 3, right). Törnvall et al (2005) found that the range of

motion of THOR's shoulder was less than that of the human shoulder by a factor of three. The SD-1 was designed to have more human-like shoulder geometry (Figure 2) and range-of-motion (Törnvall et al. 2007). In oblique frontal impacts, the SD-1 shoulder motion was similar to the PMHS (Törnvall et al 2008a).
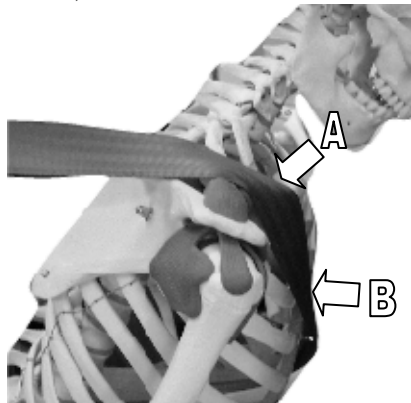

Figure 1. Diagonal shoulder belt loading the shoulder and the anterior ribcage. Normal belt forces shared by clavicle (A) and anterior ribcage (B).
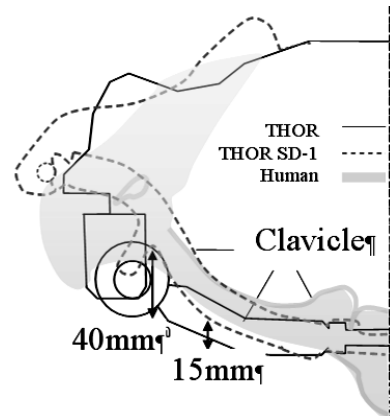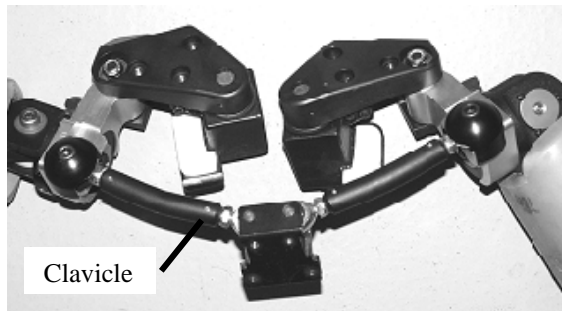

Figure 2. Shoulder comparison. Top view of right shoulder. The THOR SD-1 clavicle is 15-40 mm more posterior than THOR.

Standard THOR NT Shoulder   Chalmers SD-1 Shoulder

Figure 3. THOR NT standard shoulder and Chalmers SD-1 shoulder.

Encouraged by the apparent improved biofidelity of the SD-1, we designed a study to evaluate the shoulder's effect on ribcage deformation of the THOR dummy. More human-like thoracic deformation response would increase THOR's utility as a tool with which to assess injury potential. This study compares the thoracic response of the THOR NT frontal crash dummy with and without the SD-1 shoulder modification (labeled as THOR SD-1 and THOR, respectively, throughout this paper) to the thoracic response of Post Mortem Human Surrogates (PMHS).

METHOD

Shaw et al. (2009a, 2009b) presented PMHS thoracic response, specifically the torso deformation in response to diagonal belt loading arising from subject interaction with the restraint system, from sled tests simulating a 40 km/h frontal crash. These tests included eight male PMHS with approximately 50th percentile stature and mass (Table 1).

Table 1. PMHS Characteristics

Test:	1294	1295	1358	1359	1360	1378	1379	1380	Ave.	Std
Age	76	47	54	49	57	72	40	37	54	4.9
Mass (kg)	70	68	79	76	64	81	88	78	75.5	2.8
Stature (mm)	1780	1770	1770	1840	1750	1840	1790	1800	1793	11.6
Cause of Death	Pancreatic Cancer	Coronary Artery Disease	CVA and Atrial Fibulation	Lung Cancer	Neoplasm of Brain	Cancer	Cardiovascular Disease	Seizure Disorder		

All PMHS procurement and experimentation procedures were approved by a University of Virginia Oversight Committee established by the Vice President for Research, which functions as an institutional review board for PMHS experimentation. PMHS that were non-ambulant for an extended period prior to death were excluded, as were subjects with bony pathology in the thorax as determined from pre-test CT scans. The PMHS that were selected for testing were preserved by freezing and confirmed free of the infectious diseases HIV and Hepatitis B and C.

Following the PMHS test series, dummy tests were conducted using identical conditions (40km/h frontal crash pulse with a standard three-point belt) using the 50th percentile male THOR NT dummy. The THOR NT is the most recent version of NHTSA's advanced frontal crash test dummy (Shams et al 2005). Two configurations of the dummy were tested, one with the standard THOR shoulders installed, and one with the Chalmers University SD-1 shoulders installed. Two replicate tests were conducted with each version of the dummy.

TEST FIXTURE: The test fixture (Figure 4) was designed to provide a reasonable approximation of real world frontal impact crash loading of a belted occupant while providing repeatable and reproducible test conditions that yielded torso response data suitable for analysis.
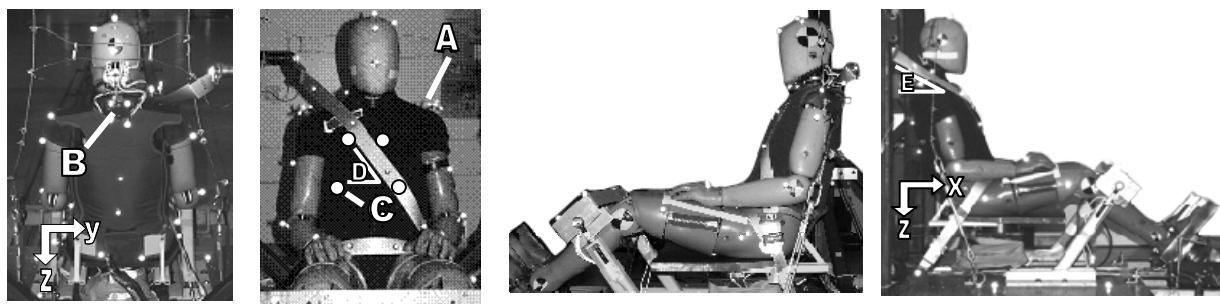

Figure 4. Test fixture and THOR NT pre-test. Markers for the point tracking system were mounted to the shoulders (A) and to the posterior surface of the upper spine box (B). Approximate CRUX positions (C). Belt angle across chest (D). Belt angle from anchor to top of shoulder (E).

The subjects were positioned on a rigid planar seat with their torso and head supported by an adjustable matrix of cables to approximate the seated posture of a right front passenger (Figure 4). The restraint consisted of a custom 3-point shoulder and lap belt with anchor positions approximating those found in the front passenger seat in a typical mid-size U.S. sedan. Each section of the belt was separately adjustable for length and joined near the subject's left hip, a location approximating that of a stalk–mounted buckle. Neither belt segment included a retractor. Pelvis and lower extremity movements were restricted by a stiff (aluminum) knee bolster adjusted to be in contact with the proximal tibias at the time of impact and by an aluminum footrest with ankle straps. The combination of a snug lap belt, the stiff, channeled knee bolster, and the stiff footrest was designed to minimize pelvic and lower extremity movements during the event while allowing the forward torso pitch characteristic of an actual automotive restraint system.

INSTRUMENTATION: Kinematic measurements, including the torso deformation of PMHS, were collected at 1000Hz using an optoelectronic stereophotogrammetric system (OSS) consisting of 16 Vicon MX™ cameras that tracked the position of retro reflective spherical markers in a calibrated 3D space lying within the cameras' collective field of view. Four-marker clusters were secured to the spine, shoulders, and anterior ribcage to facilitate the determination of the position and orientation of the corresponding bone using rigid body mechanics and coordinate transformations at each time step (Shaw et al 2009a).

THOR torso deformation was recorded at four sites by CRUX instrumentation which provided 3-D motion of the anterior ribcage relative to the spine (Figure 5) (Rangarajan et al 1998).
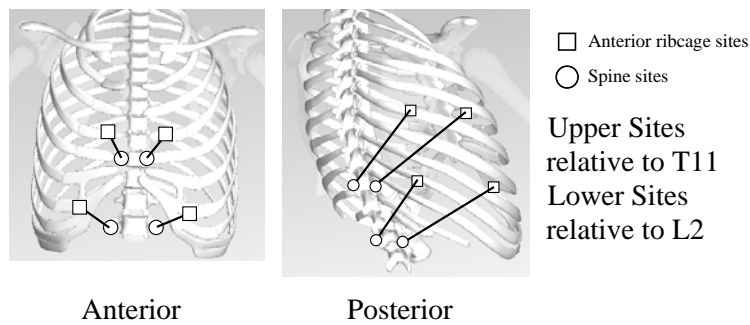
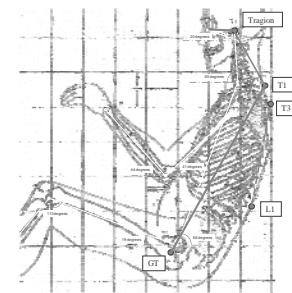Figure 5. Torso deformation measurement sites.

Figure 6. UMTRI driver position

SUBJECT POSITIONING: The position and torso orientation of all eight subjects relative to the restraint system was similar. The torso angle target was defined by the UMTRI driver position (Figure 6). For the PMHS, this angle was measured as the inclination from vertical of a line between the first thoracic vertebra (T1) and the first lumbar vertebra (L1). This position was replicated for THOR by adjusting the lumbar mechanism to the "slouched" position and reclining the torso until the head plane was horizontal with the neck in the neutral position (NHTSA 2005a).

MEASUREMENT SITES AND PRE TEST BELT POSITION: The marker clusters on the anterior ribs of the PMHS were mounted in the same general position as the THOR CRUXs (Figures 4 and 5). The diagonal shoulder belt was oriented in a similar manner for both the PMHS and the dummies (Figure 4) The shoulder belt angle across the chest relative to the horizontal was maintained within a range from 45 to 56 degrees and the belt angle from the anchor to the top of the shoulder of 24 to 29 degrees for all subjects.

TEST PROCEDURE: The subject was positioned on the midline of the seat with the knee bolsters in contact with the anterior surface of the proximal tibias. The ankle straps were secured. The head and back support, comprised of a matrix of adjustable cables (Figure 4), and the upper shoulder belt anchor were adjusted to achieve the target seated posture and corresponding relationship of shoulder to shoulder belt. The shoulder belt, tensioned to approximately 5 N, was instrumented with tension load cells above the shoulder and near the left hip. A load cell also was mounted to the lap belt, which was then tensioned to approximately 50 N.

DATA PRESENTATION: Torso motion and deformation data are reported in accordance with the SAE coordinate system (positive axes: X forward, Y to the right, Z down (Figure 4)). Motion of the shoulder was determined by recording the kinematic measurements of the OSS for the shoulder as well as several marker cluster locations on the spine. These measurements were then used to derive the motion of the shoulder relative to a spine-fixed coordinate system. Marker cluster motion recorded for T1 and T8 (eighth thoracic vertebra) was used to approximate motion of the spine at a vertebral level with minimal influence from motion of the neck, which was defined approximately at the level of T4 for the PMHS. For the dummies, the motion of the marker cluster mounted on the upper spine segment was transformed to the approximate location of the PMHS T4 vertebra.

Torso deformation was determined by relative motion between the anterior marker locations and the spine for the PMHS and by internal instrumentation for the dummies. Dummy torso deformation data (as well as shoulder belt tension data for all subjects) were collected with TDAS, an onboard data acquisition system (Diversified Technical Systems Inc.) sampling at 10,000 samples/sec. The data were hardware-filtered to 3000 Hz, debiased, filtered to SAE J211-prescribed filter classes, and truncated for presentation.

Torso deformation is described by the proportional change in chord length from the anterior ribcage measurement locations to coordinate systems located on the spine (Figure 5). In order to compare torso deformation between the THOR NT and PMHS, it was necessary to create PMHS spine coordinate systems corresponding to those used by the THOR CRUX. The PMHS upper site motions are reported relative to the two coordinate systems on either side of the spine at the T11 level, while the PMHS lower site motions are reported relative to the two coordinate systems on either side of the spine at level of L2 (second lumbar vertebra). For each site, the initial chord length value was

used to divide the values at each time step. For THOR the chord length was the CRUX "d" value. Values greater than 1 indicate that the anterior site moved away from the spinal site.

For each measurement location, the average peak change in chord length and the standard deviation were calculated for the PMHS, THOR, and THOR SD-1. The values are presented at the time of the peak average reduction chord length for 0 to 150 ms. For example, if the PMHS average maximum reduction in chord length occurred for the upper left site at 100 ms, then values at 100 ms for the other three sites are reported. Shoulder belt tension was normalized to the 50th percentile male using subject mass (Eppinger et al 1984).

RESULTS

TORSO MOTION: Although the forward pitch of the torso (rotation about the y-axis), as measured at T4, was similar for the dummies and the PMHS, there was a marked difference in peak torso yaw (rotation about the z-axis) (Figure 7). The peak average rotation of the dummies' torso, 59 degrees (THOR 46 degrees, THOR SD-1 72 degrees), was 15 degrees greater than that of the PMHS (40 degrees average, Std 23.4 degrees).
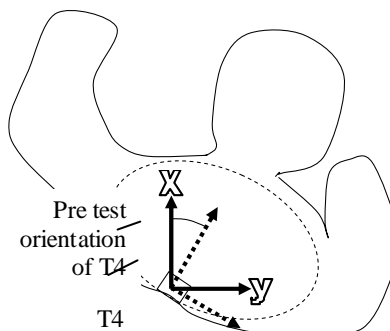

Figure 7. Torso rotation about the z axis (positive z into page).

The motion of the right shoulder relative to the spine-fixed coordinate system (Figure 8d) was greatest in the forward (x-axis) direction (Figure 8a-c). The THOR SD-1 shoulder translated forward nearly twice as far as the THOR shoulder, while all of the PMHS responses showed rearward motion of the shoulder relative to the spine.

TORSO DEFORMATION: Belt loading of the chest resulted in deformation of the anterior ribcage relative to the spine. Peak belt tension measured above the shoulder ranged from 5100 to 6700 N. Peak tension for the belt segment just above the intersection with the lap belt ranged from 4300 to 5600 N. (Figure 9). The dummy response curves exhibited a bimodal peak while most PMHS curves had a single peak at 80 to 100 ms.

Figure 10 compares the proportional change in chord lengths for the dummies and the PMHS. Figure 11 presents the average ± 1 std proportional change in chord length peak values taken at time of peak chord length reduction during the event for any one of the four sites. Figure 12 presents values calculated from the Figure 10 data. Appendix A contains a table of the peak change in chord length data for each test.

Figures 10 and 11 illustrate PMHS response that is more variable than that of the dummies. In some cases PMHS chord lengths increased during the loading event, indicating that the anterior ribcage site moves away from the spine. All PMHS exhibited this "bulge out" behavior for the lower right and at least one for the upper right and lower left.
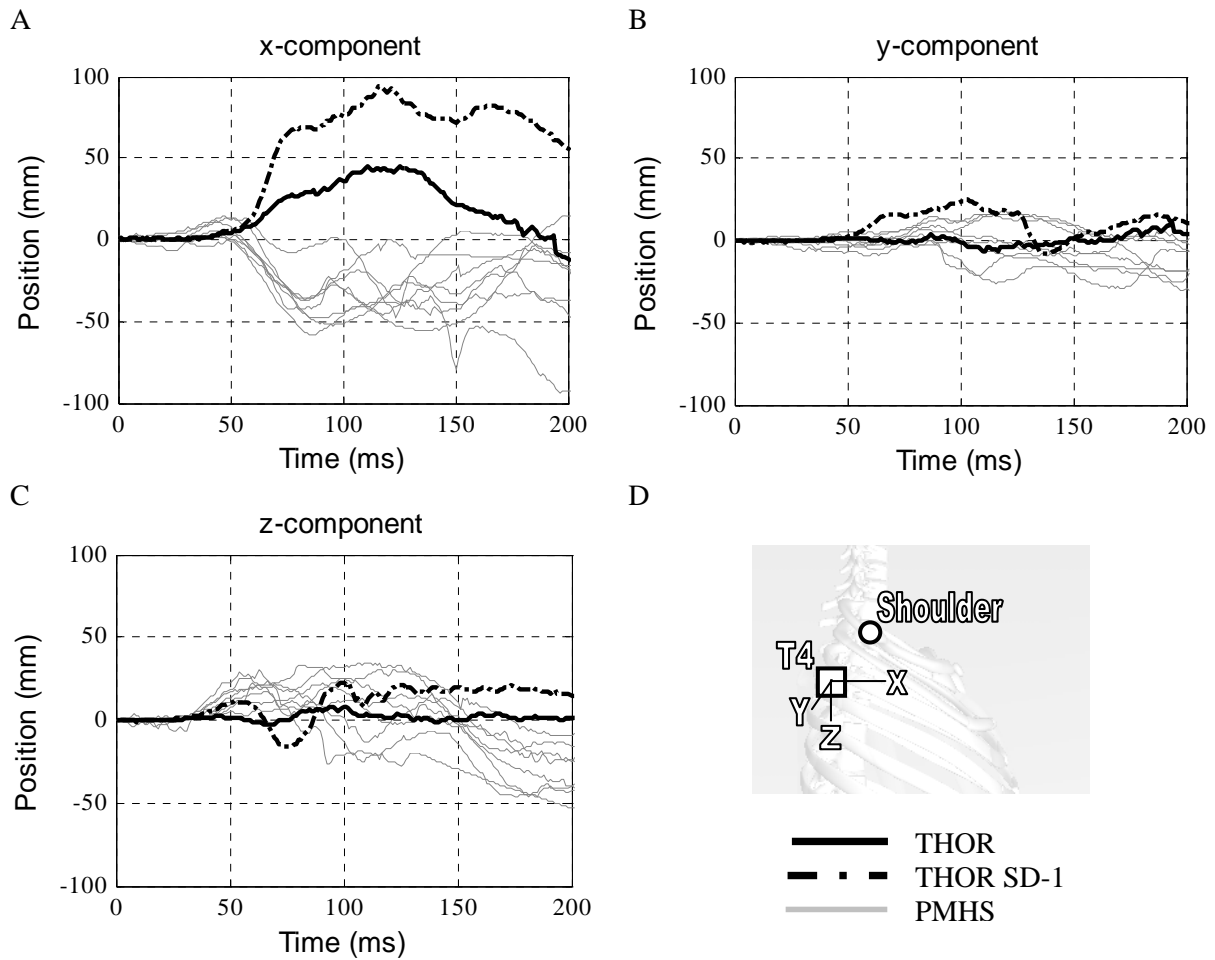
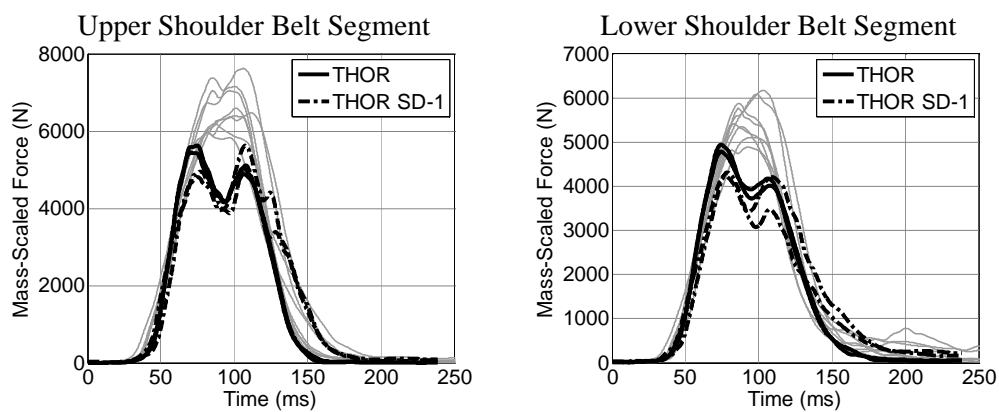**Figure 8.** Right shoulder movement relative to pre test position. Motion is relative to T4.

Figure 9. Dummy shoulder belt tension in comparison to PMHS (gray).
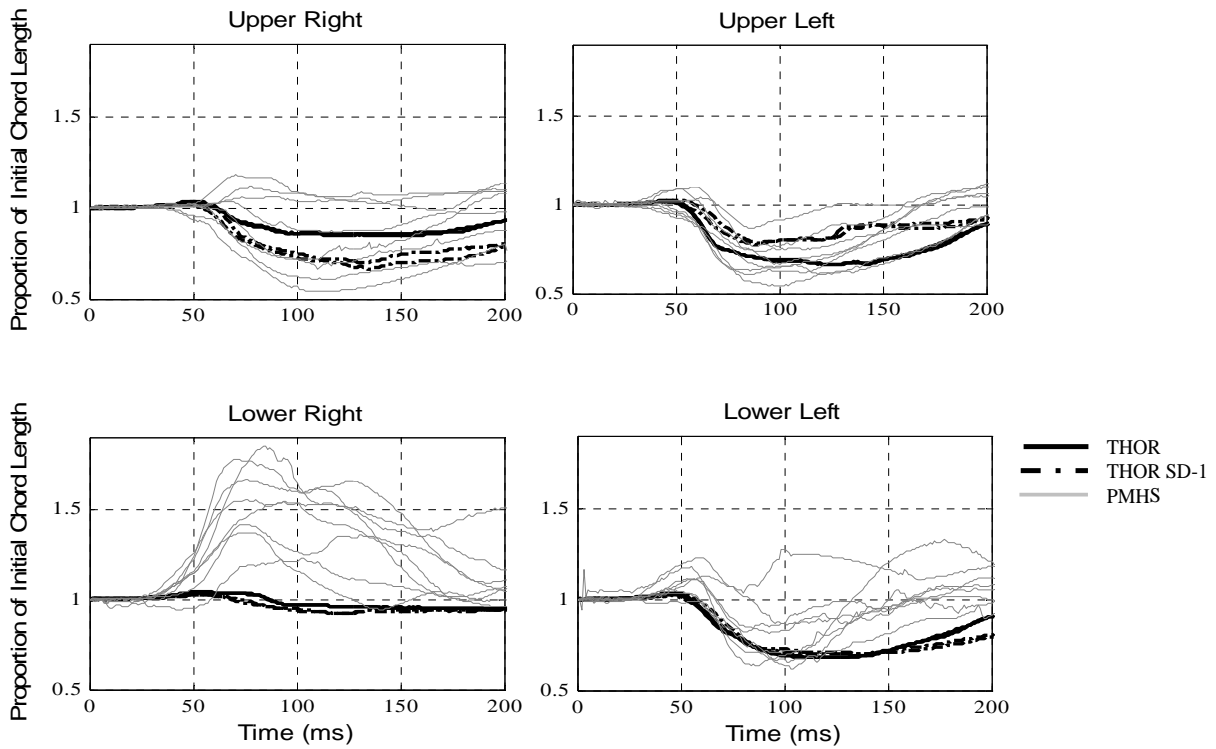
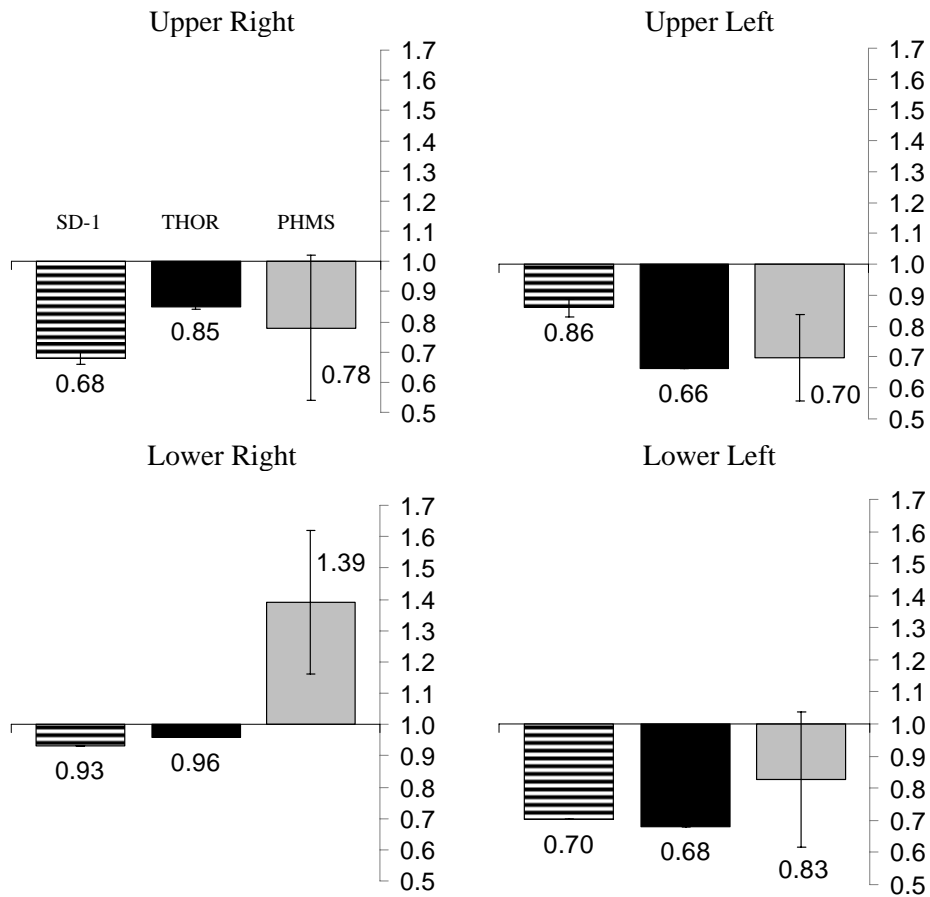**Figure 10**. Proportional change in chord length.

Figure 11. Proportional change in chord length at time of peak proportional reduction in chord length for any of the four sites. A value of "1" indicates no change. Average values for each subject are presented. Standard deviation is given for the each group of subjects.

For sites other than the lower right, the dummy and PMHS curves were generally similar and the average dummy response (THOR and THOR SD-1) was contained within 1 Std of the PMHS average for the three sites (Figures 10 and 11). However, comparing the average values (Figure 12) indicates that the dummy chord length changed more than that of the PMHS. For only the average of the upper sites was the chord length change greater for the PMHS.
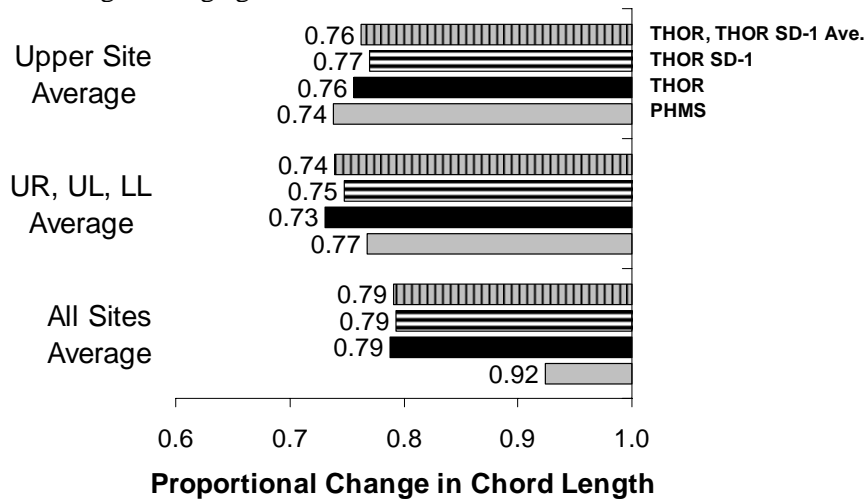

Figure 12. Proportional change in chord length averages.

For the dummies, the location of the peak chord change was reversed, upper right for THOR SD-1 and upper left for THOR. The lower site deformation was the same for both dummies as would be expected given that the modifications to the dummy were nearer to the upper CRUX sites (Figure 11).

DISCUSSION

In a frontal crash, the subject's torso continues to move forward relative to the vehicle while loading the diagonal belt with the shoulder (clavicle) and the anterior ribcage (Figure 1). The kinematically complex interaction of the torso with the belt, in the process of arresting its forward motion, produces deformation of the ribcage. The extent and pattern of ribcage deformation observed in this study is a function of several factors including torso construction, belt position, and shoulder geometry and range of motion.

BULGE OUT: The most prominent difference between the dummy and PMHS response was the motion of the lower right measurement site that moved away from the spine for the PMHS. Although forward flexion of the torso may be a contributing factor, the PMHS lower right bulge out behavior is believed to be caused primarily by inertial loading of the ribcage and underlying organs (Shaw et al 2009a, Rouhana et al 2003). THOR's thoracic cavity is essentially empty while the abdominal cavity contains lightweight fabric-covered foam structures. THOR's torso jacket is of similar lightweight construction. Therefore, the thoracic deformation response of THOR is dominated by the inertial and stiffness properties of the rib cage. The thoracic deformation response of the PMHS involves the inertial and stiffness properties of the rib cage and inertial loading by the internal organs. Additional inertial loading is provided by the soft tissues overlying the torso.

For the PMHS, these additional sources of ribcage loading resulted in movement of the anterior ribcage away from the spine at sites not restrained by the shoulder belt, a condition that made anterior ribcage motion quite sensitive to shoulder belt position relative to the measurement sites (Shaw et al 2009a). This sensitivity to belt position likely contributed to the observed variation in PMHS deformation response.

TORSO STIFFNESS: The finding that the average dummy change in chord length was greater than that recorded for the PMHS (Figure 12) suggests that the stiffness of the THOR rib cage is lower than that of PMHS. This result was unexpected given that THOR Alpha, THOR NT's predecessor, was three times stiffer than PMHS in a quasistatic indentor test (Shaw et al 2005, Shaw et al 2007), stiffer in a diagonal belt bench top loading test (Personal communication R. Kent 3/10), and stiffer in frontal sled tests (Shaw et al 2000). Although relatively minor changes were made to make THOR

NT's ribcage more compliant (Shams et al 2005), it is unlikely that this alone explains the observed results.

Differences in torso loading do not explain the less stiff dummy response. In fact, normalized peak belt tension was 12 to 23 percent lower compared to the PMHS average (Figure 9). Possible explanations for this include an increased proportion of momentum transfer through the belt restraints for the PMHS, compared to an increased proportion of momentum transfer through the knee bolster for the dummies. The reason for this may be that the dummy spine allows some mass recruitment of the torso through shear loads acting in the spine as the pelvis and femurs are arrested by knee bolster. The much more compliant and flexible PMHS spine substantially reduces mass recruitment thus requiring the belt restraints to bear the full momentum transfer of the torso. Therefore, while total momentum transfer for the subjects must be similar, the apportioning of the momentum transfer may be different for dummies and the PMHS due to structural differences in the spine. This would explain the lower belt forces and higher knee bolster forces for the dummies.

The most likely cause of the apparent discrepancy with prior studies is the difference in the method used to measure deflection. In the prior studies, THOR ribcage deflection was defined as the x-axis component of the CRUX measurement. For the PMHS, ribcage deflection was measured externally with a chestband. The chestband measurement, when corrected for skin compression, was thought to approximate the x axis movement relative to the spine comparable to CRUX "x".

When the THOR NT with the standard shoulder x-axis values are compared to the PMHS x axis values, the results are similar to those of prior studies: the dummy is stiffer than the PMHS. Figure 13 plots the average of the three anterior measurement sites that moved toward the spine, the upper right, upper left, and lower left. The change in the THOR value for x axis movement (1-0.86 = 0.14) was about half of the change in the chord value (1-0.73 = 0.27) and smaller than that of the PMHS for any measurement method, whether using the X-axis deflection or chord length with respect to either a reference frame centered at T8 or a reference frame centered at the approximate location of the anchor point of the THOR CRUX units.
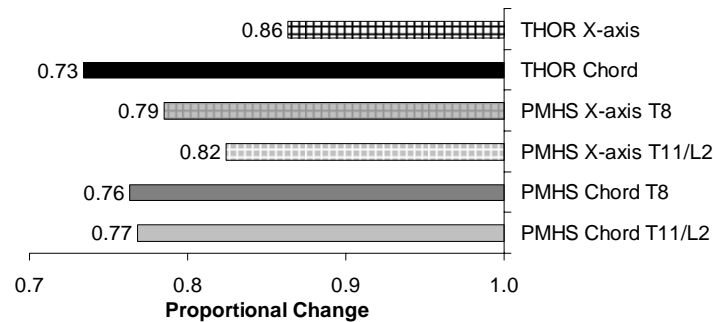

Figure 13. Proportional change in length as a function of deformation measurement method. Average of upper right, upper left, and lower left.
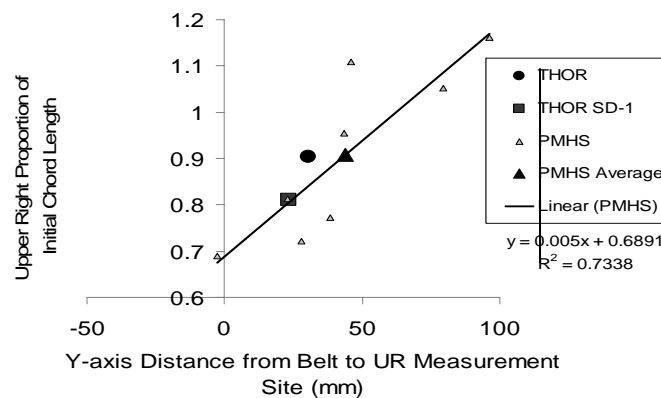

Figure 14. Relationship of distance from belt to upper right measurement site and upper right torso deformation at 80 ms.
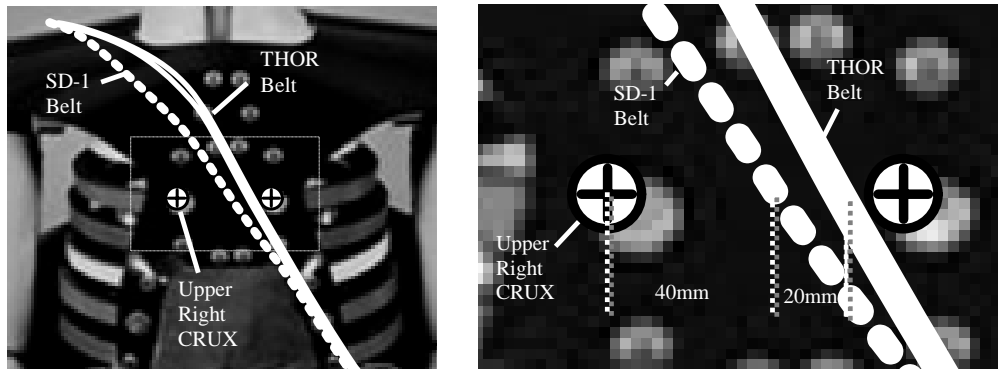
Figure 15. Shoulder belt lie pretest. The THOR SD-1 belt centerline was approximately 40 mm to the left of the right upper CRUX. The THOR belt centerline was 60 mm to the left of the right upper CRUX.

BELT POSITION: Belt position, a reported determinate of anterior ribcage deformation patterns for dummy test subjects (Horsch et al 1991) and for PMHS test subjects (Shaw et al 2009a), was related to the deformation recorded for the upper right measurement site (Figure 14) and likely was the cause of the left/right reversal of the upper measurement site peak values for the dummies. Despite similar pre-test positioning of the shoulder belt at the level of the neck/torso junction, the THOR SD-1 pre-test belt lie was approximately 20 mm closer to the right CRUX measurement location (Figure 15). A major contribution to this difference was the geometry of the THOR SD-1 clavicle, which allowed the shoulder belt to sit more lateral and posterior on the shoulder compared to the standard THOR (Figure 2). Differences in jacket geometry and materials may have contributed to the difference in belt position as well. At 120 ms, the approximate time of peak chest deformation, the belt centerline position was also about 30 mm closer to the right CRUX of the THOR SD-1 than the THOR, as estimated from reconstruction of torso and belt 3D motion from VICON measurements.

It should be noted that lateral belt position also varied as a function of time and that the movement pattern was different for each subject type. Figure 16 plots the movement of the belt relative to the spine at the level of the upper measurement sites, which corresponds to the approximate z axis location of T8. While the PMHS average belt movement was toward the right, the THOR belt moved toward the left. The THOR SD-1 belt movement pattern is similar to THOR until approximately 100 ms when it trends toward the right. Movement to the right relative to the spine also meant movement that reduced the distance between the belt and the upper right measurement site (Figure 17). The PMHS distance decreases rapidly at approximately 90 ms so that at 120 ms the average distance is 11 mm, (Std 44 mm). The THOR distance increases from 50 to 120 ms as does that of the THOR SD-1.
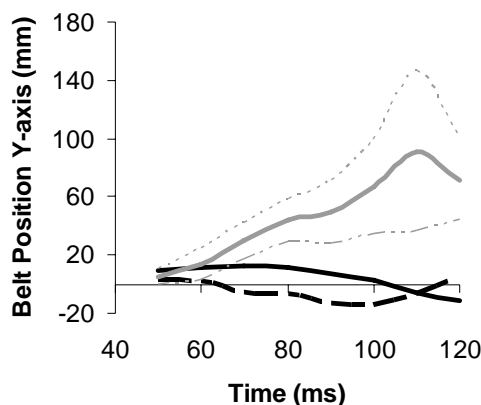

Figure 16. Lateral (y-axis) movement of the belt relative to spine at the T8 level. Positive values indicate movement to the right.
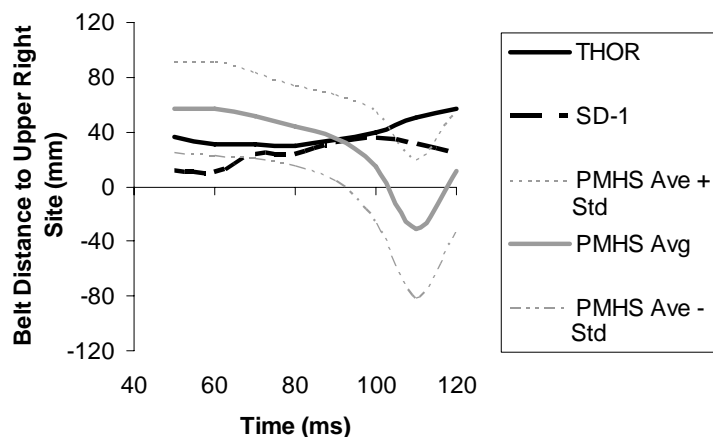
Figure 17. Lateral (y-axis) distance of the belt relative to the upper right measurement site.

While the SD-1 shoulder altered THOR's belt movement pattern, the resulting belt movement was dissimilar to that observed for the PMHS. This result was due either to the shoulder response, or, more likely, the combination response of the shoulder and torso.

The effect of the SD-1 shoulder and the resulting altered belt position could also be seen in the acceleration time histories of the upper spine segment at a level that corresponds to the human T1 (Appendix B). The THOR SD-1 x axis acceleration was approximately 15 percent lower than recorded for THOR with the standard shoulder.

SHOULDER SHIELDING: Shoulder shielding, the mechanism by which the shoulder shares a portion of the shoulder belt load, is determined by the position of the clavicle in relation to the anterior ribcage and the relative stiffness of the shoulder. In this study, because motion tracking limitations did not allow direct measurement of the dummy clavicle motion, clavicle position was assumed to be related to the position of the right shoulder. The position of the upper anterior ribcage was assumed to be related to the position of the spine at the level of T4.

Right shoulder motion was substantially different for the dummies and the PMHS. The THOR and the THOR SD-1 shoulders moved forward relative to the spine whereas the PMHS right shoulder was arrested rapidly by the belt as the thoracic cage translated forward resulting in apparent rearward shoulder motion relative to the spine. This suggests less shoulder shielding for the PMHS than for the dummies. However, the apparent reduction in PMHS shoulder shielding did not yield less upper torso deformation (Figure 10).

The geometry of the SD-1 shoulder suggested that it would provide less shoulder shielding than the original THOR NT shoulder. The section of the SD-1 clavicle under the shoulder belt is approximately 15-40 mm less anterior than the standard clavicle (Figure 2). However, the SD-1 clavicle was observed to move forward rapidly between 55 and 75 ms and that both clavicles are in approximately the same anterior-posterior location at the time of peak torso deformation. Only a modest (approximately 18 mm z-axis at the time of peak upper right thorax deformation) downward movement of the SD-1 relative to that of the standard shoulder indicates a similarly modest reduction in SD-1 shoulder shielding that, along with altered belt position, may have contributed to the greater upper right site deformation (Figure 11). Therefore, despite substantial differences in both geometry and range of motion, the SD-1 shoulder's clavicle was positioned to provide similar shoulder shielding at the time of peak torso deformation.

OBSERVATIONS

The study results suggest that torso deformation was determined more by the bulge out behavior and by shoulder belt position than by the effects of shoulder shielding. The dummy ribcage failed to demonstrate the prominent PMHS bulge out for the site farthest from the shoulder belt. Because such an anterior ribcage deformation behavior has been suggested as a fracture mechanism ((Shaw et al 2009a) the dummy may underestimate injury for the tested diagonal belt loading condition. Alternatively, in restraint conditions in which the loading is more evenly distributed, such as in airbag or four point belt systems, the bulge and its associated injury potential will be less pronounced. In these cases, the dummy may be an effective tool with which to evaluate injury potential despite torso construction that is not human-like in terms of its mass distribution and rib stiffness.

As suggested by prior studies that examined the effects of diagonal shoulder belt loading on torso deformation (Horsch et al 1991 and Schneider et al 1992), the altered belt position due to the SD-1 shoulder changed THOR's torso deformation response. However, the current study indicates that changes to the shoulder alone are insufficient to approximate PMHS torso deformation response. The SD-1 shoulder and associated jacket modifications altered THOR's chest deformation response primarily because it altered the belt path over the upper chest rather than a substantial change in shoulder shielding. Lower ribcage response and the lack of bulge out essentially were unchanged. By changing the site of the peak upper chest deflection from the upper left to the upper right, the SD-1 response was less PMHS-like in terms of average peak values (Figure 11). However, Figure 10 shows that the THOR SD-1 time-history response was similar to two of the PMHS subjects. Due to the variability of PMHS response due sensitivity to belt location exasperated by the bulge out behavior (and general subject-to-subject variability), it is difficult to identify a target PMHS response.

LIMITATIONS AND RECOMMENDATIONS

Defining torso deformation in a way that allowed comparison between the dummy and PMHS proved challenging, despite the development of coordinate systems at T11 and L2 to approximate the dummy CRUX measurement locations (see Methods). Triaxial motion of sites on the anterior ribcage relative to coordinate systems created on the spine, as presented in Shaw et al 2009a., was considered but produced results that were difficult to interpret. The rotational mobility of the PMHS spine resulted in spine coordinate systems that also rotated relative to the anterior ribcage. This rotation created apparent translations of anterior ribcage sites. In some cases, this resulted in x-axis movement, the established chest deflection metric, which did not reflect the proximity of the anterior site relative to the spine. Figure 18 illustrates how rotation of the spine-based coordinate system can result in a reduction of the x-axis motion of the anterior ribcage site when the distance between the origin of the coordinate system and the anterior site does not change. For this reason, we used the PMHS response data reported in Shaw et al 2009a. to calculate the changes in distance (chord length) between sites on the spine and anterior ribcage. This method, similar to that used for the interpretation of chestband data (Kuppa and Eppinger 1998), provides a more easily understood quantification of ribcage deformation that can be used for both the PMHS and the dummies. Although care was taken to select the same spine and anterior ribcage sites for both the PMHS and the dummies, pre test chord lengths may be somewhat different. This difference in initial chord length would affect the proportional chord length change analysis.

The chord method is but one of many ways to describe deformation and, as discussed above, different definitions of deformation can produce different conclusions regarding relative dummy and PMHS stiffness. Moreover, the Figure 13 illustrates how PMHS deformation values are affected by deformation method. For example, the average deformation metric for PMHS x axis relative to T11/L2 is 25 percent lower than that for the chord length relative to T8 (1- (-0.18/-0.24) x 100). The effect of measurement method is more evident when examining the lower right PMHS bulge out site (Figure 19). The chord analysis for the T8 spinal reference minimizes the bulge compared to the L2 spinal reference, since the chord length between the lower spine L2 and the lower right site is more affected by the upward motion of the anterior site than is the mid spine (T8) chord length (Figure 20).

While the T8 chord analysis masks the potentially injurious bulge out behavior, it may better describe the deformation of a particular rib, in this case rib 8. The lower anterior sites approximate the anterior extremities of the 8th ribs.

Although the chord length deformation method chosen for this study effectively describes movement of the anterior ribcage relative to the spine in a way that allows PMHS comparison with the THOR CRUX, further investigation is required to develop a method that best characterizes torso deformation in a way that can be related to ribcage fracture, a necessary prerequisite for the development of dummy torso response design targets.

A – Spinal rotation.
B – Spine-based coordinate system.
C – Anterior ribcage measurement site (distance to the spine coordinate system origin remains constant).
X_o – Initial x-axis value.
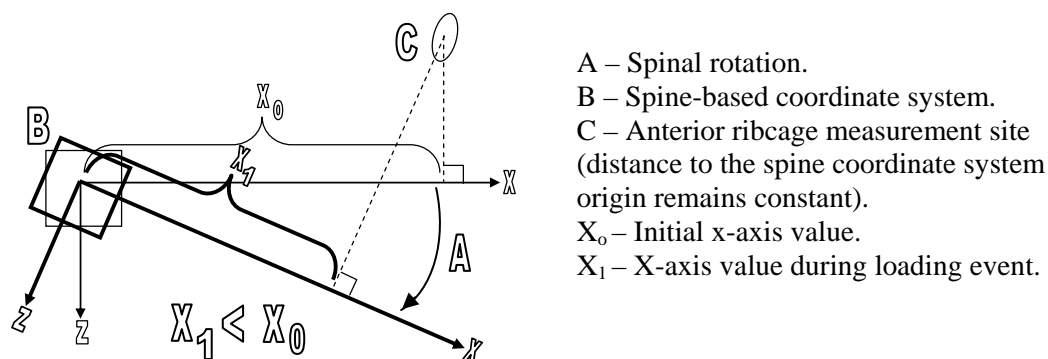X_1 – X-axis value during loading event.

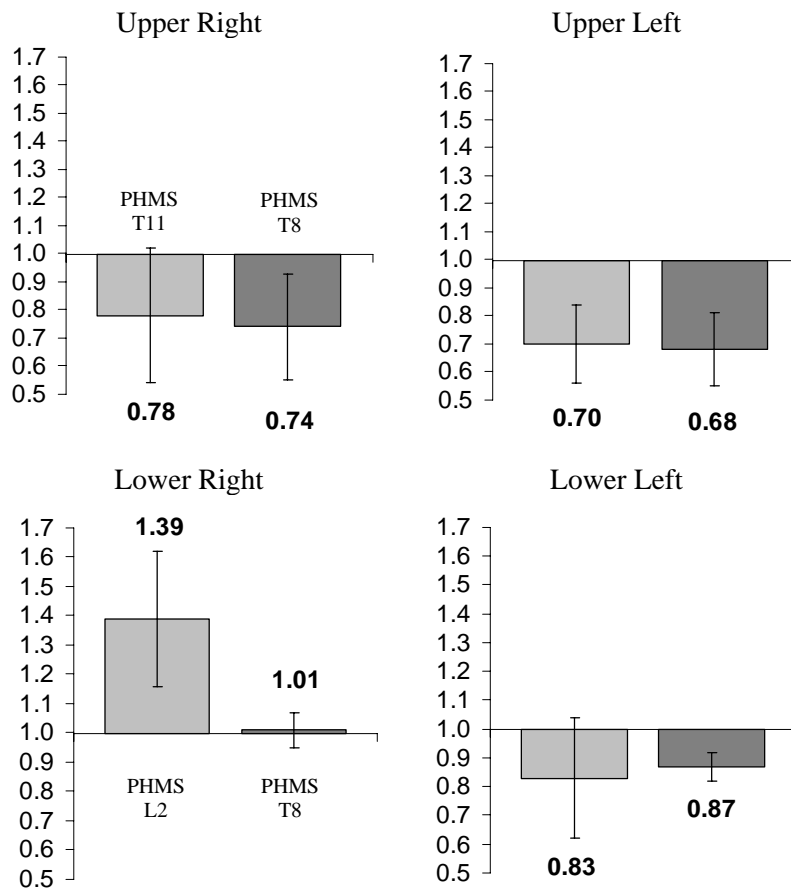**Figure 18**. Effect of spinal rotation on x-axis motion.

Figure 19. Average proportional change in chord length with standard deviation for T11 and T8 vertebral references for the upper sites and for L2 and T8 for the lower sites. Proportional change in chord length at time of peak proportional reduction in chord length for any of the four sites. Y-axis = (Peak Value + Initial Length) / Initial Length
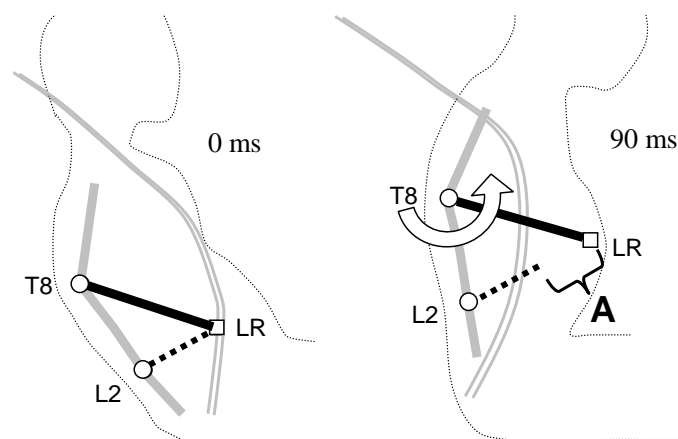

Figure 20. Chord length changes of the lower right (LR) anterior ribcage measurement site relative to the T8 and L2 vertebrae at time T zero and at 90 ms. The motion of LR, away from the spine and upward, involves little change in the T8-LR chord. The upward movement of LR results in an increased length (A) of the L2-LR chord.

For both the dummy to PMHS and the THOR to THOR SD-1 comparisons, the study results provide limited evidence of the effects of shoulder shielding on torso deformation. It is possible that the test conditions that limited forward torso rotation (pitch about the y-axis) relative to contemporary force-limited belt systems produced a loading pattern that reduced the effect of the shoulder shielding mechanism. Further study is required to understand the complex interaction of the shoulder and torso and how the simplified dummy torso and shoulder structures can be best configured to approximate human response during belt loading.

Since the SD-1 shoulder's forward motion relative to the spine was not similar to the PMHS, the developers have adjusted the shoulder's range of motion. The modified shoulder, the SD-2, provides the capability of rearward motion as was consistently observed for the PMHS (Törnvall 2008b).

SUMMARY

This study evaluated the thorax deformation response of THOR NT dummy with and without a prototype shoulder, the Chalmers SD-1, in comparison to eight male PMHS. All subjects were restrained by a three point belt and subjected to a simulated 40 km/h frontal impact.

Care should be taken when interpreting the deformation results. The chord deformation analysis chosen for this study indicated that the dummy thorax was softer than the PMHS, in apparent contradiction of prior investigations. However, the analysis method used in the prior investigations produced deformation results consistent with the prior findings.

Although the SD-1 shoulder changed the dummy deformation pattern, primarily by altering the shoulder belt path over the upper torso, the change was not sufficient to produce torso deformation that approximated the PMHS. While this study provides information concerning how shoulder modifications might change torso deformation response, the method used to compare dummy to PMHS is but one of many ways to define deformation. Further work is required to develop a deformation metric that best reflects injury potential and that can be used as a design criterion for dummy torso performance.

ACKNOWLEDGEMENTS

REFERENCES

Eppinger, R, Marcus, J, Morgan, R. Development of Dummy and Injury Index for NHTSA's Thoracic Side Impact Protection Research Program. Paper 840885, Society of Automotive Engineers (SAE), 1984.

Horsch JD; Melvin JW; Viano DC; Mertz HJ. Thoracic Injury Assessment of Belt Restraint Systems Based On Hybrid III Chest Compression. Stapp Car Crash Conference Proceedings, Paper 912895, 1991.

Kent, RW, Sherwood, CP, Lessley, DJ, Overby, B, Matsuoka, F. Age-related changes in the effective stiffness of the human thorax using four loading conditions. IRCOBI Conference on the Biomechanics of Impact, 2003.

Kent, RW, Henary, BY, Matsuoka, F. On the fatal crash experience of older drivers. Annual Proceedings/Association for the Advancement of Automotive Medicine, 49: 371-391, 2005.

Kuppa, S, Eppinger. R. Development of an Improved Thoracic Injury Criterion. Stapp Car Crash Conference Proceedings, Paper 983153, 1998.

Morris, A, Welsh, R, Frampton, R, Charlton, J, Fildes, B. An overview of requirements for the crash protection of older drivers. Annual Proceedings/Association for the Advancement of Automotive Medicine (AAAM), 46: 141-156, 2002.

NHTSA\GESAC. THOR-NT User's Manual. 50% Male Frontal Dummy. Revision 2005.1, March 2005. Report No: GESAC-05-02, 2005a

Nirula R; Pintar FA. Identification of Vehicle Components Associated With Severe Thoracic Injury in Motor Vehicle Crashes: a CIREN and NASS Analysis. Accident Analysis and Prevention, 40(1): 137-141, 2008.

Rangarajan, N., Shams, T., McDonald, J., White, R., Oster, J., Hjerpe, E., Haffner, M. Response of THOR in frontal sled testing in different restraint conditions. IRCOBI Conference on the Biomechanics of Impact, 1998.

Rouhana SW; Bedewi PG; Kankanala SV; Prasad P; Zwolinski JJ; Meduvsky AG; Rupp JD; Jeffreys TA; Schneider LW. Biomechanics of 4-Point Seat Belt Systems in Frontal Impacts. Stapp Car Crash Journal, 47: 367-399, 2003.

Schneider, LW, Ricci, L, Salloum, MJ, Beebe, MS, King, AI, Rouhana, SW, Neathery, RF. Design and development of an advanced ATD thorax system for frontal crash environments. Final report volume 1: primary concept development. Trauma assessment device development program. DOT HS 808 138. Pgs 196, 203-206, Appendix A, June 1992.

Shams T, Rangarajan N, McDonald J, Wang Y, Spade C, Pope P, Haffner M. Development of THOR-NT: enhancement of THOR Alpha-the NHTSA advanced frontal dummy. International Technical Conference on the Enhanced Safety of Vehicles (ESV), 18th, 2005.

Shaw, CG, Crandall, JR, Butcher, J. Biofidelity Evaluation of the THOR Advanced Frontal Crash Test Dummy. IRCOBI Conference on the Biomechanics of Impact, 2000.

Shaw, CG, Lessley, DJ, Kent, RW, Crandall, JR. Dummy Torso Response to Anterior Quasi-Static Loading. Paper 05-0371, Proceedings of the 19th International Technical Conference on the Enhanced Safety of Vehicles (ESV), 2005.

Shaw, CG, Lessley, DJ, Evans, J, Crandall, JR, Shin, J, Portier, P, Paoloni, G. Quasi-static and dynamic thoracic loading tests: cadaveric torsos. IRCOBI Conference on the Biomechanics of Impact, 2007.

Shaw, CG, Parent, DP, Purtsezov, S, Lessley, DJ, Crandall, JR, Kent, RW, Guillemot, H, Ridella, SA, Takhounts, E, Martin, P. Impact Response of Restrained PMHS in Frontal Sled Tests: Skeletal Deformation Patterns Under Seat Belt Loading. Stapp Car Crash Journal, 53, 1-48, 2009a.

Shaw, CG, Parent, DP, Purtsezov, S, Lessley, DJ, Kerrigan, JR, Shin, J, Crandall, JR, Zama, Y, Ejima, S, Kamiji, K, Yasuki, T. Frontal Impact PMHS Sled Tests for FE TORSO Model Development. IRCOBI Conference on the Biomechanics of Impact, 2009b.

Törnvall FV; Holmgvist K; Martinsson J; Davidsson J. Comparison of Shoulder Range-Of-Motion and Stiffness Between Volunteers, Hybrid III and Thor Alpha in Static Frontal Impact Loading. International Journal of Crashworthiness, 10(2): 151-160, 2005.

Törnvall, FV., Holmqvist, K., Davidsson, J., Svensson, M. Y., Håland, Y. and Öhrn, H. A New THOR Shoulder Design: A Comparison with Volunteers, the Hybrid III and THOR NT. Traffic Injury Prevention, 8(2): 205–215, 2007.

Tornvall, FV Holmqvist, K, Davidsson, J, Svensson, M, Gugler, J, Steffan, H, Haland, Y. (2008) Evaluation of Dummy Shoulder Kinematics in Oblique Frontal Collisions. IRCOBI Conference on the Biomechanics of Impact, 2008a

Tornvall, FV. A New Shoulder for the THOR Dummy Intended for Oblique Collisions. Doctoral Thesis. Chalmers University of Technology, Goteborg, Sweden, 2008b.

Appendix A Torso Deformation Test Data
Proportional Change Values

CHORD		Upper Right		Upper Left		Lower Right		Lower Left	
Site	Spine Location:	T11	T8	T11	T8	L2	T8	L2	T8
	Test Number								
THOR	1286	0.86		0.66		0.96		0.68	
	1287	0.85		0.66		0.96		0.68	
	avg	**0.85**		**0.66**		**0.96**		**0.68**	
	std	0.01		0.00		0.00		0.00	
THOR SD-1	1289	0.69		0.84		0.93		0.70	
	1290	0.67		0.88		0.94		0.70	
	avg	**0.68**		**0.86**		**0.93**		**0.70**	
	std	0.02		0.03		0.00		0.00	
PMHS	1294	0.75	0.69	0.63	0.67	1.63	1.06	0.63	0.90
	1295	0.56	0.50	0.54	0.55	1.27	0.92	0.64	0.84
	1358	1.06	0.96	0.60	0.61	1.51	1.08	0.70	0.86
	1359	0.66	0.63	0.94	0.84	1.53	1.00	1.25	0.89
	1360	0.60	0.67	0.75	0.76	1.43	1.03	0.90	0.90
	1378	1.25	1.07	0.66	0.71	1.60	1.08	0.83	0.83
	1379	0.69	0.63	0.61	0.50	1.13	0.97	0.69	0.79
	1380	0.66	0.73	0.86	0.83	1.02	0.98	0.97	0.96
	avg	**0.78**	**0.74**	**0.70**	**0.68**	**1.39**	**1.01**	**0.83**	**0.87**
	std	0.24	0.19	0.14	0.13	0.23	0.06	0.21	0.05
X AXIS									
	Test Number								
THOR	1286	0.93		0.83		0.98		0.84	
	1287	0.92		0.82		0.98		0.83	
	avg	**0.93**		**0.82**		**0.98**		**0.83**	
	std	0.00		0.00		0.00		0.01	
THOR SD-1	1289	0.79		0.94		0.96		0.83	
	1290	0.77		0.95		0.96		0.82	
	avg	**0.78**		**0.95**		**0.96**		**0.83**	
	std	0.02		0.01		0.00		0.00	
PMHS	1294	0.76	0.76	0.79	0.75	1.25	1.21	0.98	0.84
	1295	0.55	0.60	0.65	0.64	1.16	1.08	0.78	0.66
	1358	0.94	0.93	0.67	0.66	1.27	1.20	0.87	0.76
	1359	0.66	0.72	0.94	0.91	1.11	1.16	1.10	0.86
	1360	0.68	0.73	0.81	0.81	1.19	1.20	0.98	0.82
	1378	1.12	1.08	0.79	0.77	1.29	1.23	0.91	0.88
	1379	0.74	Nm	0.68	0.67	0.97	1.04	0.81	0.73
	1380	0.74	0.80	0.85	0.83	0.98	1.13	0.98	0.84
	avg	**0.77**	**0.80**	**0.77**	**0.75**	**1.15**	**1.16**	**0.93**	**0.80**
	std	0.16	0.14	0.09	0.08	0.11	0.06	0.09	0.07

Appendix B THOR Upper Spine Segment Acceleration